DESY 96-140
UdeM-GPP-TH-96-38
July 1996

CP Violation and Flavour Mixing in the Standard Model – 1996 Update

A. Ali[1]

Deutsches Elektronen Synchrotron DESY, Hamburg

and

D. London[2]

Physics Department, McGill University
3600 University St., Montréal, Québec, Canada, H3A 2T8

Abstract

We review and update the constraints on the parameters of the quark flavour mixing matrix V_{CKM} in the standard model and estimate the resulting CP asymmetries in B decays, taking into account recent experimental and theoretical developments. With the updated CKM matrix we present the currently-allowed range of the ratios $|V_{td}/V_{ts}|$ and $|V_{td}/V_{ub}|$, as well as the standard model predictions for the B_s^0-$\overline{B_s^0}$ mixing parameter x_s (or, equivalently, ΔM_s) and the quantities $\sin 2\alpha$, $\sin 2\beta$ and $\sin^2\gamma$, which characterize the CP-asymmetries in B-decays.

[1]Presented at the QCD Euroconference 96, Montpellier, July 4 - 12, 1996.

[2]Permanent address: Laboratoire de physique nucléaire, Université de Montréal, C.P. 6128, succ. centre-ville, Montréal, QC, Canada H3C 3J7.

1 An Update of the CKM Matrix

We revise and update the profile of the Cabibbo-Kobayashi-Maskawa (CKM) matrix [1] reported by us in 1995 [2]. In particular, we focus on the CKM unitarity triangle and CP asymmetries in B decays, which are the principal objects of interest in experiments at present and forthcoming B facilities. In performing this update, we include the improvements reported in a number of measurements of the lifetime, mixing ratio, and the CKM matrix elements $|V_{cb}|$ and $|V_{ub}/V_{cb}|$ from B decays, as well as the top quark mass, $|\epsilon|$, and progress in theoretical calculations involving a number of perturbative and non-perturbative aspects of QCD.

In updating the CKM matrix elements, we make use of the Wolfenstein parametrization [3], which follows from the observation that the elements of this matrix exhibit a hierarchy in terms of λ, the Cabibbo angle. In this parametrization the CKM matrix can be written approximately as

$$V_{CKM} \simeq \begin{pmatrix} 1-\frac{1}{2}\lambda^2 & \lambda & A\lambda^3(\rho - i\eta) \\ -\lambda(1+iA^2\lambda^4\eta) & 1-\frac{1}{2}\lambda^2 & A\lambda^2 \\ A\lambda^3(1-\rho-i\eta) & -A\lambda^2 & 1 \end{pmatrix} . \tag{1}$$

We shall discuss those quantities which constrain these CKM parameters, pointing out the significant changes in the determination of λ, A, ρ and η, as compared to [2]. Also, for reasons of brevity, we shall be rather concise in this report and refer to [4, 2] for further details.

We recall that $|V_{us}|$ has been extracted with good accuracy from $K \to \pi e \nu$ and hyperon decays [5] to be

$$|V_{us}| = \lambda = 0.2205 \pm 0.0018 . \tag{2}$$

This agrees quite well with the determination of $V_{ud} \simeq 1 - \frac{1}{2}\lambda^2$ from β-decay [5],

$$|V_{ud}| = 0.9736 \pm 0.0010 . \tag{3}$$

We note and comment on the changes that we have made in the input to our present analysis compared to that reported by us last year in Ref. [2]:

- m_t: The present average of the top quark mass measured directly at Fermilab by the CDF and D0 collaborations is $m_t = 175 \pm 9$ GeV [6]. We interpret this as being the pole mass (though this identification is not unambiguous). This, in turn, leads to the running top quark mass in the $\overline{MS}$ scheme, $\overline{m_t}(m_t) = 165 \pm 9$ GeV [7].

- $|V_{cb}|$: The determination of $|V_{cb}|$ from inclusive and exclusive B decays has been reviewed earlier in a number of studies [2, 8, 9, 10]. Here, we shall concentrate on the exclusive decay $B \to D^* \ell \nu_\ell$ analyzed in the context of heavy quark effective theory (HQET), as this method seems to have been scrutinized in great detail. Using HQET, the differential decay rate in $B \to D^* \ell \nu_\ell$ is [11]

$$\frac{d\Gamma(B \to D^* \ell \bar{\nu})}{d\omega} = \frac{G_F^2}{48\pi^3}(m_B - m_{D^*})^2 m_{D^*}^3 \eta_A^2 \sqrt{\omega^2 - 1}(\omega + 1)^2 \times [1 + \frac{4\omega}{\omega + 1}\frac{1 - 2\omega r + r^2}{(1 - r)^2}]|V_{cb}|^2 \xi^2(\omega) \ , \quad (4)$$

where $r = m_{D^*}/m_B$, $\omega = v \cdot v'$ (v and v' are the four-velocities of the B and D^* meson, respectively), and η_A is the short-distance correction to the axial vector form factor. Measurements of the intercept $\mathcal{F}(1)|V_{cb}|$ (with $\mathcal{F}(\omega) \equiv \eta_A \cdot \xi(\omega)$) in the decays $B \to D^* \ell \nu_\ell$, have been reported by the ALEPH, ARGUS, DELPHI, CLEO, and OPAL collaborations, and a careful job of averaging the experimental results on the intercept $\mathcal{F}(1)|V_{cb}|$ has been performed for the presently available data by Gibbons [12]. The intercept is highly correlated with the slope of the Isgur-Wise function $\mathcal{F}(y)$ [11] measured in each experiment and a simultaneous average of the slope and the intercept is required with the correlations included. We refer to Ref. [12] for the details of the analysis, and quote the final result, which reads as

$$\mathcal{F}(1)|V_{cb}| = 0.0357 \pm 0.0020 \pm 0.0014, \quad (5)$$

where the first error is statistical plus systematic, and the second is the estimate of the curvature bias in extrapolating the function $\mathcal{F}(y)$. Theoretical estimates for the quantity $\mathcal{F}(1)$ are on a firmer footing, as the QCD perturbative part η_A has been calculated at next-to-leading order in Ref. [13], yielding $\eta_A = 0.965 \pm 0.007 + \mathcal{O}({\alpha_s}^3)$, which reduces the perturbative QCD error on η_A by a factor 3, as compared to the earlier estimates of the same. (See, for example, the work by M. Neubert [8].) The remaining theoretical uncertainty is now in the power corrections to the Isgur-Wise function at the symmetry point $\xi(1)$. The leading power corrections to $\xi(1)$ are absent due to Luke's theorem [14]. There exist extensive studies of the $1/M_Q^2$ corrections and we refer to [8, 9, 15] for detailed discussions of the corrections and their model dependence. Using these estimates gives:

$$\xi(1) = 1 + \delta(1/m^2) = 0.945 \pm 0.025 \implies \mathcal{F}(1) = 0.907 \pm 0.026 \ . \quad (6)$$

The present theoretical error $\Delta\mathcal{F}(1)/\mathcal{F}(1) = 0.029$ (which appears to us to be rather irreducible) is about 2/3 the size of the theoretical error used in our earlier CKM fits [2], where we had used $\mathcal{F}(1) = 0.91 \pm 0.04$.

Taking into account the updated experimental [12] and theoretical [13] input, the present determination of $|V_{cb}|$ is:

$$|V_{cb}| = 0.0393 \pm 0.0021\ (expt) \pm 0.0015\ (curv) \pm 0.0011\ (th), \qquad (7)$$

In the fits below we have added the errors in quadrature, getting

$$|V_{cb}| = 0.0393 \pm 0.0028\ , \qquad (8)$$

yielding

$$A = 0.81 \pm 0.058\ . \qquad (9)$$

This represents a measurement of this parameter at $\pm 7.2\%$, making it after λ the next best determined CKM parameter. We note that the central value of A is essentially the same as that used in [2], but the error is now reduced.

- $|V_{ub}/V_{cb}|$: The knowledge of the CKM matrix element ratio $|V_{ub}/V_{cb}|$ is based on the analysis of the end-point lepton energy spectrum in semileptonic decays $B \to X_u \ell \nu_\ell$ and the measurement of the exclusive semileptonic decays $B \to (\pi, \rho) \ell \nu_\ell$ reported by the CLEO collaboration [10]. As noted in [16], the inclusive measurements suffer from a large extrapolation factor from the measured end-point rate to the total branching ratio, which is model dependent. The exclusive measurements allow a discrimination among a number of models [10], all of which were previously allowed from the inclusive decay analysis alone. It is difficult to combine the exclusive and inclusive measurements to get a combined determination of $|V_{ub}|/|V_{cb}|$. However, it has been noted that the disfavoured models in the context of the exclusive decays are also those which introduce a larger theoretical dispersion in the interpretation of the inclusive $B \to X_u \ell \nu_\ell$ data. Excluding them from further consideration, measurements in both the inclusive and exclusive modes are compatible with [12]:

$$\left|\frac{V_{ub}}{V_{cb}}\right| = 0.08 \pm 20\%\ . \qquad (10)$$

This gives

$$\sqrt{\rho^2 + \eta^2} = 0.363 \pm 0.073\ . \qquad (11)$$

Again, the central value of this quantity is the same as that used by us in [2], but the error is marginally reduced.

- $|\epsilon|, \hat{B}_K,$ and constraints on ρ and η: The experimental value of $|\epsilon|$ has changed somewhat from our previous analyses, and the error has decreased [5]:

$$|\epsilon| = (2.280 \pm 0.013) \times 10^{-3}\ . \qquad (12)$$

Theoretically, $|\epsilon|$ is essentially proportional to the imaginary part of the box diagram for K^0-$\overline{K^0}$ mixing and is given by [17]

$$|\epsilon| = \frac{G_F^2 f_K^2 M_K M_W^2}{6\sqrt{2}\pi^2 \Delta M_K} \hat{B}_K \left(A^2\lambda^6\eta\right) \left(y_c \left\{\hat{\eta}_{ct} f_3(y_c, y_t) - \hat{\eta}_{cc}\right\} + \hat{\eta}_{tt} y_t f_2(y_t) A^2\lambda^4(1-\rho)\right), \quad (13)$$

where $y_i \equiv m_i^2/M_W^2$, and the functions f_2 and f_3 can be found in Ref. [4]. Here, the $\hat{\eta}_i$ are QCD correction factors, calculated at next-to-leading order in [18] ($\hat{\eta}_{cc}$), [19] ($\hat{\eta}_{tt}$) and [20] ($\hat{\eta}_{ct}$). The theoretical uncertainty in the expression for $|\epsilon|$ is in the renormalization-scale independent parameter $\hat{B}_K$, which represents our ignorance of the hadronic matrix element $\langle K^0|(\overline{d}\gamma^\mu(1-\gamma_5)s)^2|\overline{K^0}\rangle$. Some recent calculations of $\hat{B}_K$ using lattice QCD methods [21] and the $1/N_c$ approach [22] are: $\hat{B}_K = 0.83 \pm 0.03$ (Sharpe [23]), $\hat{B}_K = 0.86 \pm 0.15$ (APE Collaboration [24]), $\hat{B}_K = 0.67 \pm 0.07$ (JLQCD Collaboration [25]), $\hat{B}_K = 0.78 \pm 0.11$ (Bernard and Soni [25]), and $\hat{B}_K = 0.70 \pm 0.10$ (Bijnens and Prades [22]). They strongly suggest that the theoretical dispersion on this quantity has been greatly reduced compared to the ranges $\hat{B}_K = 0.8 \pm 0.2$ and $\hat{B}_K = 0.6 \pm 0.2$, which we had used previously as the best estimates in the Lattice-QCD and chiral perturbation theory frameworks, respectively. The more recent calculations given above are compatible with the range

$$\hat{B}_K = 0.75 \pm 0.10, \quad (14)$$

which we now use in our analysis. This is one of the principal sources of reduction in the allowed values of ρ and η, as we shall see later.

- $\Delta M_d, f_{B_d}^2 \hat{B}_{B_d}$, and constraints on ρ and η: From a theoretical point of view we prefer to use the mass difference ΔM_d, as it liberates one from the errors on the lifetime measurement. The present world average for ΔM_d is [12]

$$\Delta M_d = 0.464 \pm 0.018 \ (ps)^{-1} \ . \quad (15)$$

The mass difference ΔM_d is calculated from the B_d^0-$\overline{B_d^0}$ box diagram. Unlike the kaon system, where the contributions of both the c- and the t-quarks in the loop are important, this diagram is dominated by t-quark exchange:

$$\Delta M_d = \frac{G_F^2}{6\pi^2} M_W^2 M_B \left(f_{B_d}^2 \hat{B}_{B_d}\right) \hat{\eta}_B y_t f_2(y_t) |V_{td}^* V_{tb}|^2 \ , \quad (16)$$

where, using Eq. 1, $|V_{td}^* V_{tb}|^2 = A^2\lambda^6[(1-\rho)^2 + \eta^2]$. Here, $\hat{\eta}_B$ is the QCD correction. In Ref. [19], this correction was analyzed including the effects of a heavy t-quark. It was found that $\hat{\eta}_B$ depends sensitively on the definition of the t-quark mass, and that, strictly speaking, only

the product $\hat{\eta}_B(y_t) f_2(y_t)$ is free of this dependence. In the fits presented here we use the value $\hat{\eta}_B = 0.55$, calculated in the $\overline{MS}$ scheme, following Ref. [19]. Consistency requires that the top quark mass be rescaled from its pole (mass) value of $m_t = 175 \pm 9$ GeV to the value $\overline{m_t}(m_t(pole))$ in the $\overline{MS}$ scheme, given above.

For the B system, the hadronic uncertainty is given by $f_{B_d}^2 \hat{B}_{B_d}$, analogous to $\hat{B}_K$ in the kaon system, except that in this case f_{B_d} has not been measured. The present status of the lattice-QCD estimates for f_{B_d}, $\hat{B}_{B_d}$ and related quantities for the B_s meson, obtained in the quenched (now usually termed as the valence) approximation was summarized recently in [27], giving

$$\begin{aligned} f_{B_d} &= 170^{+55}_{-50} \text{ MeV}, \\ \hat{B}_{B_d} &= 1.02^{+0.05}_{-0.06} \ {}^{+0.03}_{-0.02}, \end{aligned} \tag{17}$$

where the first error on $\hat{B}_{B_d}$ is statistical and the second systematic, estimated by the UKQCD collaboration [28]. The effect of unquenching is an estimated 10% increase in the value of f_{B_d} (likewise f_{B_s}) [29]. A modern estimate of $f_{B_d}^2 \hat{B}_{B_d}$ in the QCD sum rule approach is that given in [30], which is stated in terms of f_π, and on using $f_\pi = 132$ MeV translates into

$$f_{B_d} \sqrt{\hat{B}_{B_d}} = 197 \pm 18 \text{ MeV} , \tag{18}$$

In our fits, we will take

$$f_{B_d} \sqrt{\hat{B}_{B_d}} = 200 \pm 40 \text{ MeV} , \tag{19}$$

which is compatible with the results from both lattice-QCD and QCD sum rules for this quantity. We note that the range (19) is considerably tighter as compared to our previous theoretical estimates of the same, namely $f_{B_d} \sqrt{\hat{B}_{B_d}} = 180 \pm 53$ MeV. This is the second most important source of reduction in the allowed CKM parameter space.

- ΔM_s, $\Delta M_s / \Delta M_d$ and constraints on the unitarity triangle: We also estimate the SM prediction for the B_s^0-$\overline{B_s^0}$ mixing parameter, ΔM_s and x_s. The experimental lower limits on these quantities have steadily increased, thanks to the experiments at LEP [31, 32] and more recently also from SLC. These limits have now started to be significant for the allowed CKM parameter space. The present best limit from a single experiments comes from ALEPH, $\Delta M_s > 7.8$ (ps)$^{-1}$ [32, 26]. However, combining this with the corresponding limit from DELPHI yields $\Delta M_s > 9.2$ (ps)$^{-1}$ [12], leading to $\Delta M_s / \Delta M_d > 19.0$ (95% C.L.). We show how this limit constrains the CKM parameter space. We also give the present 95% C.L. upper and lower bounds on the matrix element ratio $|V_{td}/V_{ts}|$, as well as the allowed (correlated) values of the CKM matrix elements $|V_{td}|$ and $|V_{ub}|$.

As in our previous analysis, we consider two types of fits. In Fit 1, we assume particular fixed values for the theoretical hadronic quantities. The allowed ranges for the CKM parameters are derived from the (Gaussian) errors on experimental measurements only. In Fit 2, we assign a central value plus an error (treated as Gaussian) to the theoretical quantities. In the resulting fits, we combine the experimental and theoretical errors in quadrature. For both fits we calculate the allowed region in CKM parameter space at 95% C.L.

We also present the corresponding allowed ranges for the CP-violating phases that will be measured in B decays, characterized by $\sin 2\beta$, $\sin 2\alpha$ and $\sin^2\gamma$. These can be measured directly through rate asymmetries in the decays $\overset{(-)}{B}{}^0_d \to J/\psi K_S$, $\overset{(-)}{B}{}^0_d \to \pi^+\pi^-$, and $\overset{(-)}{B}{}^0_s \to D_s^{\pm}K^{\mp}$ (or $B^{\pm} \to \overset{(-)}{D}{}^0 K^{\pm}$), respectively. We also show the allowed correlated domains for two of the CP asymmetries $(\sin 2\alpha, \sin 2\beta)$, as well as the correlation between α and γ.

This paper is organized as follows. In Section 2, we present the results of our updated fits for the CKM parameters. These results are summarized in terms of the allowed domains of the unitarity triangle, which are displayed in several figures and tables. In Section 3, we discuss the impact of the recent lower limit on the ratio $\Delta M_s/\Delta M_d$ reported by the ALEPH collaboration on the CKM parameters and estimate the expected range of the mixing ratio x_s and ΔM_s in the SM based on our fits. Here we also present the allowed 95% C.L. range for $|V_{td}/V_{ts}|$. In Section 4 we discuss the predictions for the CP asymmetries in the neutral B meson sector and calculate the correlations for the CP violating asymmetries proportional to $\sin 2\alpha$, $\sin 2\beta$ and $\sin^2\gamma$. We present here the allowed values of the CKM matrix elements $|V_{td}|$ and $|V_{ub}|$. Section 5 contains a summary and an outlook for improving the profile of the CKM unitarity triangle.

2 The Unitarity Triangle

The allowed region in ρ-η space can be displayed quite elegantly using the so-called unitarity triangle. The unitarity of the CKM matrix leads to the following relation:

$$V_{ud}V_{ub}^* + V_{cd}V_{cb}^* + V_{td}V_{tb}^* = 0 \ . \tag{20}$$

Using the form of the CKM matrix in Eq. 1, this can be recast as

$$\frac{V_{ub}^*}{\lambda V_{cb}} + \frac{V_{td}}{\lambda V_{cb}} = 1 \ , \tag{21}$$

which is a triangle relation in the complex plane (i.e. ρ-η space), illustrated in Fig. 1. Thus, allowed values of ρ and η translate into allowed shapes of the unitarity triangle.

In order to find the allowed unitarity triangles, the computer program MINUIT is used to fit the CKM parameters A, ρ and η to the experimental values of $|V_{cb}|$, $|V_{ub}/V_{cb}|$, $|\epsilon|$ and x_d. Since λ is very well measured, we have

Parameter	Value
λ	0.2205
$\lvert V_{cb}\rvert$	0.0393 ± 0.0028
$\lvert V_{ub}/V_{cb}\rvert$	0.08 ± 0.016
$\lvert\epsilon\rvert$	$(2.280 \pm 0.013) \times 10^{-3}$
ΔM_d	$(0.464 \pm 0.018)\ (ps)^{-1}$
$\tau(B_d)$	$(1.55 \pm 0.04)\ (ps)$
$\overline{m_t}(m_t(pole))$	(165 ± 9) GeV
$\hat{\eta}_B$	0.55
$\hat{\eta}_{cc}$	1.38
$\hat{\eta}_{ct}$	0.47
$\hat{\eta}_{tt}$	0.57
$\hat{B}_K$	0.75 ± 0.1
$f_{B_d}\sqrt{\hat{B}_{B_d}}$	200 ± 40 MeV

Table 1: Parameters used in the CKM fits. Values of the hadronic quantities $\hat{B}_K$ and $f_{B_d}\sqrt{\hat{B}_{B_d}}$ shown are motivated by lattice QCD results, QCD sum rules and chiral perturbation theory. In Fit 1, specific values of these hadronic quantities are chosen, while in Fit 2, they are allowed to vary over the given ranges.

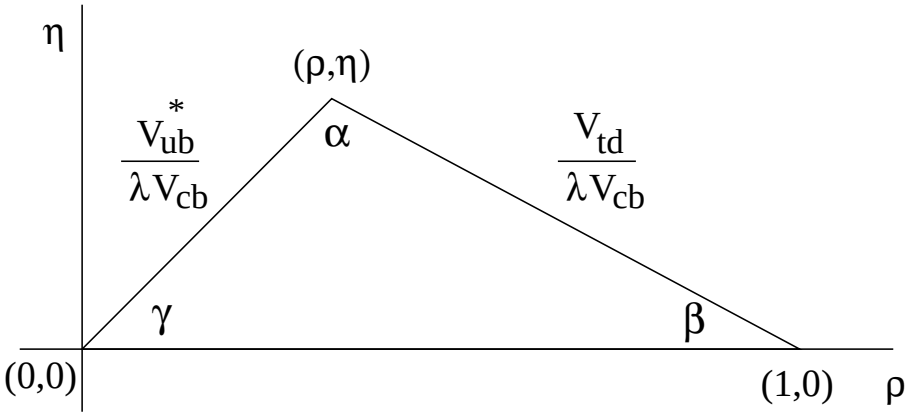

Figure 1: The unitarity triangle. The angles α, β and γ can be measured via CP violation in the B system.

$f_{B_d}\sqrt{\hat{B}_{B_d}}$ (MeV)	(ρ, η)	χ^2_{min}
130	$(-0.37,\ 0.20)$	2.53
140	$(-0.32,\ 0.24)$	0.94
150	$(-0.27,\ 0.27)$	0.23
160	$(-0.21,\ 0.30)$	1.4×10^{-2}
170	$(-0.15,\ 0.33)$	1.0×10^{-3}
180	$(-0.08,\ 0.35)$	2.8×10^{-2}
190	$(0.0,\ 0.36)$	7.9×10^{-3}
200	$(0.07,\ 0.36)$	1.6×10^{-2}
210	$(0.13,\ 0.37)$	0.20
220	$(0.19,\ 0.37)$	0.70
230	$(0.24,\ 0.37)$	1.61
240	$(0.29,\ 0.37)$	2.97

Table 2: The "best values" of the CKM parameters (ρ, η) as a function of the coupling constant $f_{B_d}\sqrt{\hat{B}_{B_d}}$, obtained by a minimum χ^2 fit to the experimental data. We fix $\hat{B}_K = 0.75$. The resulting minimum χ^2 values from the MINUIT fits are also given.

fixed it to its central value given above. As discussed in the introduction, we present here two types of fits:

- Fit 1: the "experimental fit." Here, only the experimentally measured numbers are used as inputs to the fit with Gaussian errors; the coupling constants $f_{B_d}\sqrt{\hat{B}_{B_d}}$ and $\hat{B}_K$ are given fixed values.
- Fit 2: the "combined fit." Here, both the experimental and theoretical numbers are used as inputs assuming Gaussian errors for the theoretical quantities.

We first discuss the "experimental fit" (Fit 1). The goal here is to restrict the allowed range of the parameters (ρ, η) for given values of the coupling constants $f_{B_d}\sqrt{\hat{B}_{B_d}}$ and $\hat{B}_K$. For each value of $\hat{B}_K$ and $f_{B_d}\sqrt{\hat{B}_{B_d}}$, the CKM parameters A, ρ and η are fit to the experimental numbers given in Table 1 and the χ^2 is calculated.

First, we fix $\hat{B}_K = 0.75$, and vary $f_{B_d}\sqrt{\hat{B}_{B_d}}$ in the range 130 MeV to 240 MeV. The resulting χ^2_{min} values are given in Table 2, together with the best-fit values of the CKM parameters (ρ, η). We note that for this value of $\hat{B}_K$, certain values of $f_{B_d}\sqrt{\hat{B}_{B_d}}$ are disfavoured since they do not provide a good fit to the data. Since we have two variables (ρ and η), we use $\chi^2_{min} < 2.0$ as our "good fit" criterion, and we find that $f_{B_d}\sqrt{\hat{B}_{B_d}} \leq 130$ MeV and $f_{B_d}\sqrt{\hat{B}_{B_d}} \geq 240$ MeV give poor fits to the existing data. As the allowed range of $f_{B_d}\sqrt{\hat{B}_{B_d}}$ from this fit has a large overlap with the

theoretically motivated range given above, we note that present data do not allow a further reduction of this uncertainty. The fits are presented as an allowed region in ρ-η space at 95% C.L. ($\chi^2 = \chi^2_{min} + 6.0$). The results are shown in Fig. 2. As we pass from Fig. 2 (top left) to Fig. 2 (bottom right), the unitarity triangles represented by these graphs become more and more obtuse. However, the range of possibilities for these triangles is now considerably reduced as compared to the earlier fits we have presented in [2]. This is due in part to the (somewhat) improved measurements of $|V_{cb}|$ and $|V_{ub}/V_{cb}|$, but mainly reflects our reduced theoretical errors on the quantities $\hat{B}_K$ and $f^2_{B_d}\hat{B}_{B_d}$. We hope that this trust in the improved calculational ability of these parameters is well placed! There are two things to be learned from this fit. First, our quantitative knowledge of the unitarity triangle is at present not very solid. This will be seen more clearly when we present the results of Fit 2. Second, unless our knowledge of hadronic matrix elements improves considerably, measurements of $|\epsilon|$ and x_d, no matter how precise, will not help much in further constraining the unitarity triangle. This is why measurements of CP-violating rate asymmetries in the B system are so important [33, 34]. Being largely independent of theoretical uncertainties, they will allow us to accurately pin down the unitarity triangle. With this knowledge, we could deduce the correct values of $\hat{B}_K$ and $f_{B_d}\sqrt{\hat{B}_{B_d}}$, and thus rule out or confirm different theoretical approaches to calculating these hadronic quantities.

We now discuss the "combined fit" (Fit 2). Since the coupling constants are not known and the best we have are estimates given in the ranges in Eqs. (14) and (19), a reasonable profile of the unitarity triangle at present can be obtained by letting the coupling constants vary in these ranges. The resulting CKM triangle region is shown in Fig. 3. As is clear from this figure, the allowed region is still rather large at present. However, present data and theory do restrict the parameters ρ and η to lie in the following range:

$$\begin{aligned} 0.20 \leq \eta \leq 0.52, \\ -0.35 \leq \rho \leq 0.35\ . \end{aligned} \tag{22}$$

The preferred values obtained from the "combined fit" are

$$(\rho, \eta) = (0.05, 0.36) \quad (\text{with } \chi^2 = 6.6 \times 10^{-3})\ , \tag{23}$$

which gives rise to an almost right-angled unitarity triangle, with the angle γ being close to 90 degrees. However, as we quantify below, the allowed ranges of the CP violating angles α, β, and γ estimated at the 95% C.L. are still quite large, though correlated.

3 ΔM_s (and x_s) and the Unitarity Triangle

Mixing in the B^0_s-$\overline{B^0_s}$ system is quite similar to that in the B^0_d-$\overline{B^0_d}$ system. The B^0_s-$\overline{B^0_s}$ box diagram is again dominated by t-quark exchange, and the mass

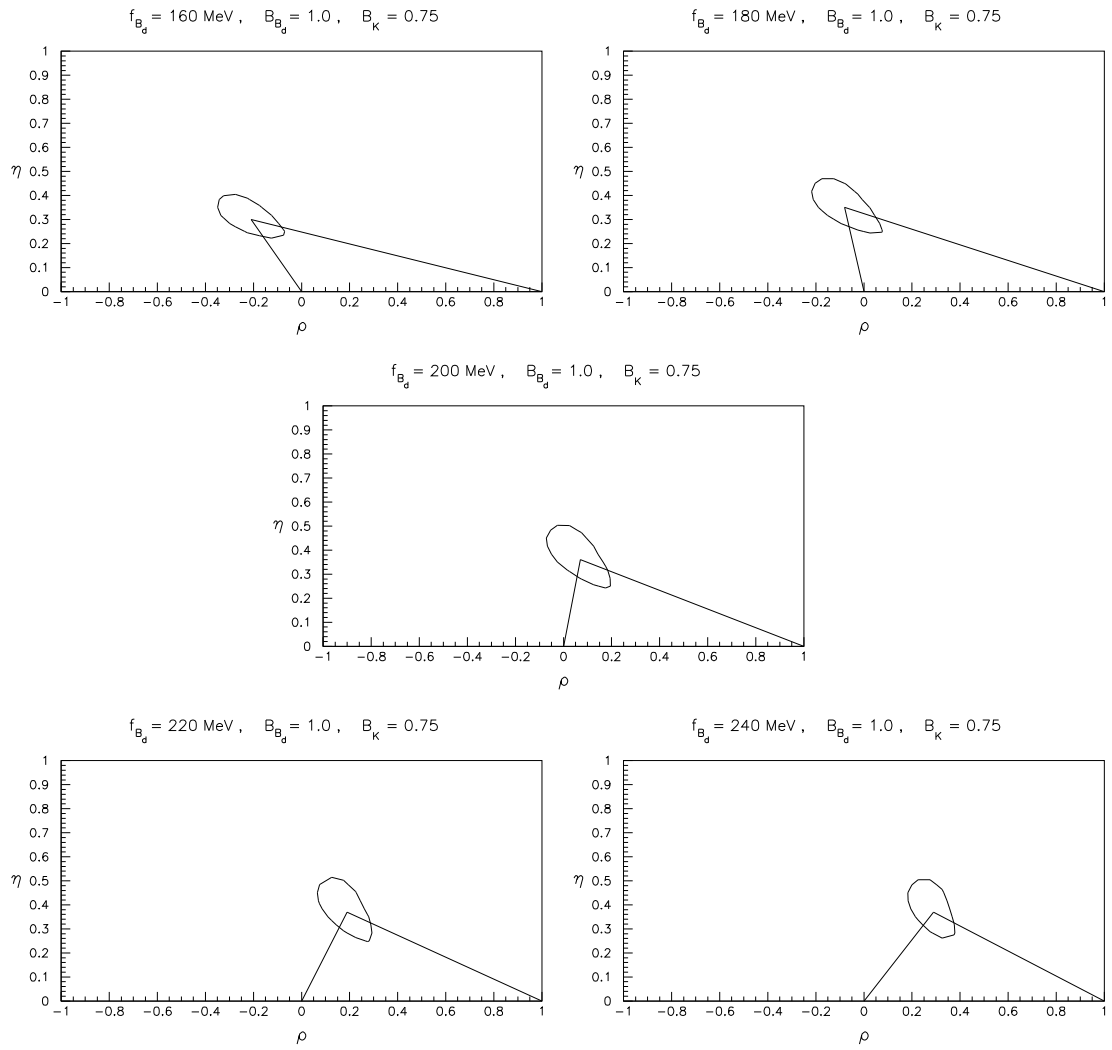

Figure 2: Allowed region in ρ-η space, from a fit to the experimental values given in Table 1. We have fixed $\hat{B}_K = 0.75$ and vary the coupling constant product $f_{B_d}\sqrt{\hat{B}_{B_d}}$ as indicated on the figures. The solid line represents the region with $\chi^2 = \chi^2_{min}+6$ corresponding to the 95% C.L. region. The triangles show the best fit.

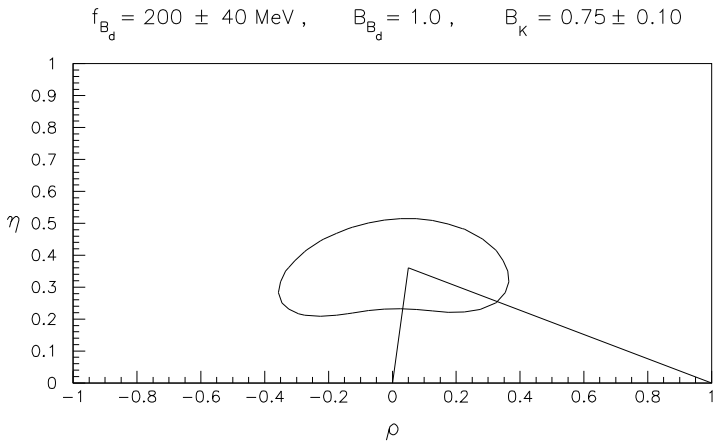

Figure 3: Allowed region in ρ-η space, from a simultaneous fit to both the experimental and theoretical quantities given in Table 1. The theoretical errors are treated as Gaussian for this fit. The solid line represents the region with $\chi^2 = \chi^2_{min} + 6$ corresponding to the 95% C.L. region. The triangle shows the best fit.

difference between the mass eigenstates ΔM_s is given by a formula analogous to that of Eq. (16):

$$\Delta M_s = \frac{G_F^2}{6\pi^2} M_W^2 M_{B_s} \left(f_{B_s}^2 \hat{B}_{B_s} \right) \hat{\eta}_{B_s} y_t f_2(y_t) |V_{ts}^* V_{tb}|^2 \ . \tag{24}$$

Using the fact that $|V_{cb}| = |V_{ts}|$ (Eq. 1), it is clear that one of the sides of the unitarity triangle, $|V_{td}/\lambda V_{cb}|$, can be obtained from the ratio of ΔM_d and ΔM_s,

$$\frac{\Delta M_s}{\Delta M_d} = \frac{\hat{\eta}_{B_s} M_{B_s} \left(f_{B_s}^2 \hat{B}_{B_s} \right)}{\hat{\eta}_{B_d} M_{B_d} \left(f_{B_d}^2 \hat{B}_{B_d} \right)} \left| \frac{V_{ts}}{V_{td}} \right|^2 . \tag{25}$$

All dependence on the t-quark mass drops out, leaving the square of the ratio of CKM matrix elements, multiplied by a factor which reflects $SU(3)_{\rm flavour}$ breaking effects. The only real uncertainty in this factor is the ratio of hadronic matrix elements. Whether or not x_s can be used to help constrain the unitarity triangle will depend crucially on the theoretical status of the ratio $f_{B_s}^2 \hat{B}_{B_s} / f_{B_d}^2 \hat{B}_{B_d}$. In what follows, we will take $\xi_s \equiv (f_{B_s}\sqrt{\hat{B}_{B_s}})/(f_{B_d}\sqrt{\hat{B}_{B_d}}) = (1.15 \pm 0.05)$, consistent with both lattice-QCD [27] and QCD sum rules [35]. (The SU(3)-breaking factor in $\Delta M_s/\Delta M_d$ is ξ_s^2.)

The mass and lifetime of the B_s meson have now been measured at LEP and Tevatron and their present values are $M_{B_s} = 5369.3 \pm 2.0$ MeV and $\tau(B_s) = 1.52 \pm 0.07\ ps$ [36]. The QCD correction factor $\hat{\eta}_{B_s}$ is equal to its B_d counterpart, i.e. $\hat{\eta}_{B_s} = 0.55$. The main uncertainty in ΔM_s (or, equivalently, x_s) is now $f_{B_s}^2 \hat{B}_{B_s}$. Using the determination of A given previously, and

$\overline{m_t} = 165 \pm 9$ GeV, we obtain

$$\Delta M_s = (12.8 \pm 2.1)\, \frac{f_{B_s}^2 \hat{B}_{B_s}}{(230\ \text{MeV})^2}\ (ps)^{-1}\ ,$$
$$x_s = (19.5 \pm 3.3)\, \frac{f_{B_s}^2 \hat{B}_{B_s}}{(230\ \text{MeV})^2}\ . \tag{26}$$

The choice $f_{B_s}\sqrt{\hat{B}_{B_s}} = 230$ MeV corresponds to the central value given by the lattice-QCD estimates, and with this our fits give $x_s \simeq 20$ as the preferred value in the SM. Allowing the coefficient to vary by $\pm 2\sigma$, and taking the central value for $f_{B_s}\sqrt{\hat{B}_{B_s}}$, this gives

$$12.9 \le x_s \le 26.1\ ,$$
$$8.6\ (ps)^{-1} \le \Delta M_s \le 17.0\ (ps)^{-1}\ . \tag{27}$$

It is difficult to ascribe a confidence level to this range due to the dependence on the unknown coupling constant factor. All one can say is that the standard model predicts large values for ΔM_s (and hence x_s). The present experimental limit $\Delta M_s > 9.2\ (ps)^{-1}$ [12] is marginally better than the lower bound on this quantity given above.

An alternative estimate of ΔM_s (or x_s) can also be obtained by using the relation in Eq. (25). Two quantities are required. First, we need the CKM ratio $|V_{ts}/V_{td}|$. In Fig. 4 we show the allowed values (at 95% C.L.) of the inverse of this ratio as a function of $f_{B_d}\sqrt{\hat{B}_{B_d}}$, for $\hat{B}_K = 0.75 \pm 0.1$. From this one gets

$$2.94 \le \left|\frac{V_{ts}}{V_{td}}\right| \le 6.80\ . \tag{28}$$

We note in passing that unitarity of the CKM matrix constrains this ratio to be $3.0 \le |V_{ts}/V_{td}| \le 9.1$ (this can be obtained from Eq. 21, along with the experimental values of λ and $|V_{ub}/V_{cb}|$.)

The second ingredient is the SU(3)-breaking factor which we take to be $\xi_s = 1.15 \pm 0.05$, or $1.21 \le \xi_s^2 \le 1.44$. The result of the CKM fit can therefore be expressed as a 95% C.L. range:

$$11.4 \left(\frac{\xi_s}{1.15}\right)^2 \ \le\ \frac{\Delta M_s}{\Delta M_d}\ \le\ 61.2 \left(\frac{\xi_s}{1.15}\right)^2\ . \tag{29}$$

Again, it is difficult to assign a true confidence level to $\Delta M_s/\Delta M_d$ due to the dependence on ξ_s. However, the uncertainty due to the CKM matrix element ratio has now been reduced to a factor 5.3 due to the tighter constraints on the unitarity triangle – our previous fits [2] gave a factor 7.4. The allowed range for the ratio $\Delta M_s/\Delta M_d$ shows that this method is still poorer at present for the determination of the range for ΔM_s, as compared to the absolute value for ΔM_s discussed above, which in comparison is uncertain by a factor of 2. Both suffer from additional dependences on $f_{B_s}\sqrt{\hat{B}_{B_s}}$ or ξ_s.

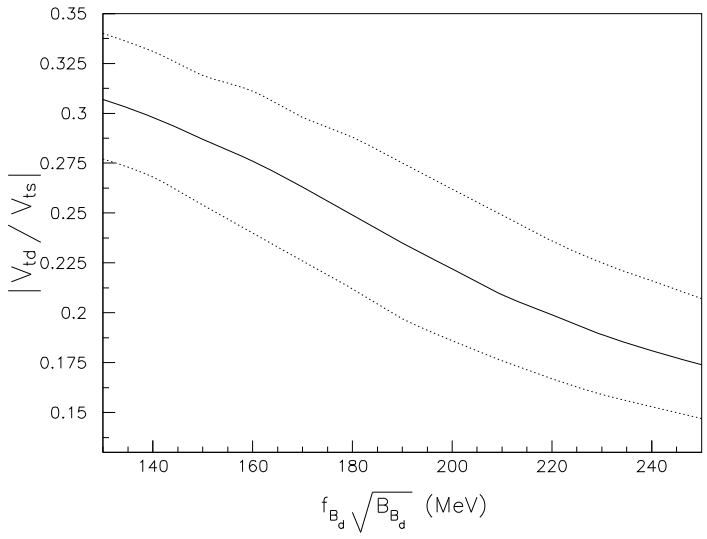

Figure 4: Allowed values of the CKM matrix element ratio $|V_{td}/V_{ts}|$ as a function of the coupling constant product $f_{B_d}\sqrt{\hat{B}_{B_d}}$, for $\hat{B}_K = 0.75 \pm 0.1$. The solid line corresponds to the best fit values and the dotted curves correspond to the maximum and minimum allowed values at 95 % C.L.

The present lower bound from LEP $\Delta M_s > 9.2\ (ps)^{-1}$ (95% C.L.) [12] and the present world average $\Delta M_d = (0.464 \pm 0.018)\ (ps)^{-1}$ can be used to put a bound on the ratio $\Delta M_s/\Delta M_d$, yielding $\Delta M_s/\Delta M_d > 19.0$. This is significantly better than the lower bound on this quantity from the CKM fits, using the central value for ξ_s. The 95% confidence limit on $\Delta M_s/\Delta M_d$ can be turned into a bound on the CKM parameter space (ρ, η) by choosing a value for the SU(3)-breaking parameter ξ_s^2. We assume three representative values: $\xi_s^2 = 1.21$, 1.32 and 1.44, and display the resulting constraints in Fig. 5. From this graph we see that the LEP bound now restricts the allowed ρ-η region for all three values of ξ_s^2, though this restriction is weakest for the largest value of ξ_s^2 assumed. This shows that the LEP bound on ΔM_s provides a more stringent lower bound on the matrix element ratio $|V_{ts}/V_{td}|$ than that obtained from the CKM fits without this constraint or that following from the unitarity of the CKM matrix.

Summarizing the discussion on x_s, we note that the lattice-QCD-inspired estimate $f_{B_s}\sqrt{\hat{B}_{B_s}} \simeq 230$ MeV and the CKM fit predict that x_s lies between 13 and 26, with a central value around 20. All of these values scale as $(f_{B_s}\sqrt{\hat{B}_{B_s}}/230\ \text{MeV})^2$. The present constraints from the lower bound on ΔM_s on the CKM parameters are now competitive with those from fits to other data, and this will become even more pronounced with improved data. In particular, one expects to reach a sensitivity for $x_s \simeq 15$ (or $\Delta M_s \simeq 10\ ps^{-1}$) at LEP combining all data and tagging techniques, and similarly at the SLC, CDF and HERA-B. Of course, an actual measurement of ΔM_s (equivalently x_s) would be very helpful in further constraining the CKM

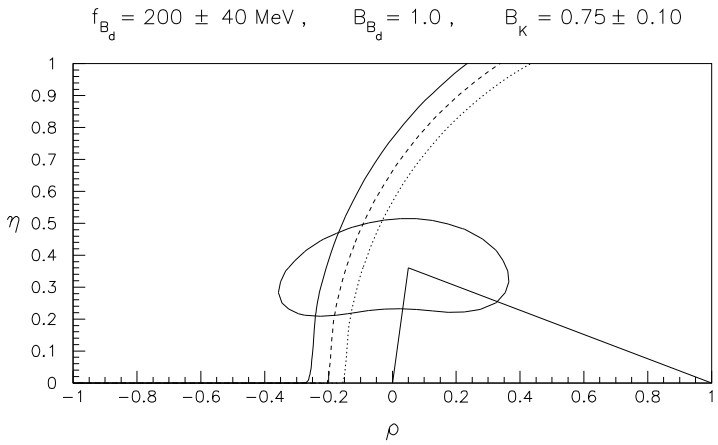

Figure 5: Further constraints in ρ-η space from the LEP bound $\Delta M_s/\Delta M_d > 19.0$. The bounds are presented for 3 choices of the SU(3)-breaking parameter: $\xi_s^2 = 1.21$ (dotted line), 1.32 (dashed line) and 1.44 (solid line). In all cases, the region to the left of the curve is ruled out.

parameter space. We note that the entire range for x_s worked out here is accessible at the LHC experiments.

4 CP Violation in the B System

It is expected that the B system will exhibit large CP-violating effects, characterized by nonzero values of the angles α, β and γ in the unitarity triangle (Fig. 1) [33]. The most promising method to measure CP violation is to look for an asymmetry between $\Gamma(B^0 \to f)$ and $\Gamma(\overline{B^0} \to f)$, where f is a CP eigenstate. If only one weak amplitude contributes to the decay, the CKM phases can be extracted cleanly (i.e. with no hadronic uncertainties). Thus, $\sin 2\alpha$, $\sin 2\beta$ and $\sin 2\gamma$ can in principle be measured in $\overset{(-)}{B_d} \to \pi^+\pi^-$, $\overset{(-)}{B_d} \to J/\psi K_S$ and $\overset{(-)}{B_s} \to \rho K_S$, respectively.

Penguin diagrams [37] will, in general, introduce some hadronic uncertainty into an otherwise clean measurement of the CKM phases. In the case of $\overset{(-)}{B_d} \to J/\psi K_S$, the penguins do not cause any problems, since the weak phase of the penguin is the same as that of the tree contribution. Thus, the CP asymmetry in this decay still measures $\sin 2\beta$. For $\overset{(-)}{B_d} \to \pi^+\pi^-$, however, although the penguin is expected to be small with respect to the tree diagram, it will still introduce a theoretical uncertainty into the extraction of α. This uncertainty can, in principle, be removed by the use of an isospin analysis [38], which requires the measurement of the rates for $B^+ \to \pi^+\pi^0$, $B^0 \to \pi^+\pi^-$ and $B^0 \to \pi^0\pi^0$, as well as their CP-conjugate counterparts. Thus, even in the presence of penguin diagrams, $\sin 2\alpha$ can in principle be extracted from the decays $B \to \pi\pi$. Still, this isospin program is ambitious

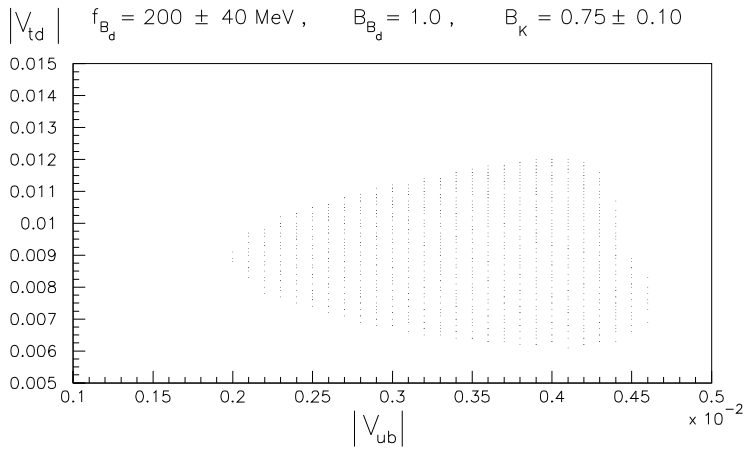

Figure 6: Allowed region of the CKM matrix elements $|V_{td}|$ and $|V_{ub}|$ resulting from the "combined fit" of the data for the ranges for $f_{B_d}\sqrt{\hat{B}_{B_d}}$ and $\hat{B}_K$ given in the text.

experimentally. If it cannot be carried out, the error induced on $\sin 2\alpha$ is of order $|P/T|$, where P (T) represents the penguin (tree) diagram. The ratio $|P/T|$ is difficult to estimate since it is dominated by hadronic physics. However, one ingredient is the ratio of the CKM elements of the two contributions: $|V_{tb}^* V_{td}/V_{ub}^* V_{ud}| \simeq |V_{td}/V_{ub}|$. From our fits, we have determined the allowed values of $|V_{td}|$ as a function of $|V_{ub}|$. This is shown in Fig. 6 for the "combined fit". The allowed range for the ratio of these CKM matrix elements is

$$1.4 \leq \left|\frac{V_{td}}{V_{ub}}\right| \leq 4.6 \ , \tag{30}$$

with a central value of about 3.

It is $\overline{(B_s)} \to \rho K_S$ which is most affected by penguins. In fact, the penguin contribution is probably larger in this process than the tree contribution. This decay is clearly not dominated by one weak (tree) amplitude, and thus cannot be used as a clean probe of the angle γ. Instead, two other methods have been devised, not involving CP-eigenstate final states. The CP asymmetry in the decay $\overline{(B_s)} \to D_s^{\pm} K^{\mp}$ can be used to extract $\sin^2\gamma$ [39]. Similarly, the CP asymmetry in $B^{\pm} \to D_{CP}^0 K^{\pm}$ also measures $\sin^2\gamma$ [40]. Here, D_{CP}^0 is a D^0 or $\overline{D^0}$ which is identified in a CP-eigenstate mode (e.g. $\pi^+\pi^-$, K^+K^-, ...).

These CP-violating asymmetries can be expressed straightforwardly in terms of the CKM parameters ρ and η. The 95% C.L. constraints on ρ and η found previously can be used to predict the ranges of $\sin 2\alpha$, $\sin 2\beta$ and $\sin^2\gamma$ allowed in the standard model. The allowed ranges which correspond to each of the figures in Fig. 2, obtained from Fit 1, are found in Table 3. In this table we have assumed that the angle β is measured in $\overline{(B_d)} \to J/\Psi K_S$, and have therefore included the extra minus sign due to the CP of the final

$f_{B_d}\sqrt{\hat{B}_{B_d}}$ (MeV)	$\sin 2\alpha$	$\sin 2\beta$	$\sin^2\gamma$
160	0.86 – 1.0	0.38 – 0.58	0.47 – 0.92
180	−0.05 – 1.0	0.47 – 0.71	0.77 – 1.0
200	−0.69 – 0.90	0.53 – 0.81	0.61 – 1.0
220	−0.85 – 0.61	0.60 – 0.89	0.44 – 0.98
240	−0.90 – 0.32	0.67 – 0.94	0.34 – 0.86

Table 3: The allowed ranges for the CP asymmetries $\sin 2\alpha$, $\sin 2\beta$ and $\sin^2\gamma$, corresponding to the constraints on ρ and η shown in Fig. 2. Values of the coupling constant $f_{B_d}\sqrt{\hat{B}_{B_d}}$ are stated. We fix $\hat{B}_K = 0.75$. The range for $\sin 2\beta$ includes an additional minus sign due to the CP of the final state $J/\Psi K_S$.

state.

Since the CP asymmetries all depend on ρ and η, the ranges for $\sin 2\alpha$, $\sin 2\beta$ and $\sin^2\gamma$ shown in Table 3 are correlated. That is, not all values in the ranges are allowed simultaneously. We illustrate this in Fig. 7, corresponding to the "experimental fit" (Fit 1), by showing the region in $\sin 2\alpha$-$\sin 2\beta$ space allowed by the data, for various values of $f_{B_d}\sqrt{\hat{B}_{B_d}}$. Given a value for $f_{B_d}\sqrt{\hat{B}_{B_d}}$, the CP asymmetries are fairly constrained. However, since there is still considerable uncertainty in the values of the coupling constants, a more reliable profile of the CP asymmetries at present is given by our "combined fit" (Fit 2), where we convolute the present theoretical and experimental values in their allowed ranges. The resulting correlation is shown in Fig. 8. From this figure one sees that the smallest value of $\sin 2\beta$ occurs in a small region of parameter space around $\sin 2\alpha \simeq 0.8$-0.9. Excluding this small tail, one expects the CP-asymmetry in $\overset{(-)}{B}_d \to J/\Psi K_S$ to be at least 20% (i.e., $\sin 2\beta > 0.4$). Finally, in the SM the relation $\alpha + \beta + \gamma = \pi$ is satisfied. However, note that the allowed range for β is rather small (Table 3). Thus, there should be a strong correlation between α and γ [41]. This is indeed the case, as is shown in Fig. 9.

5 Summary and Outlook

We summarize our results:

(i) We have presented an update of the CKM unitarity triangle using the theoretical and experimental improvements in the following quantities: $|\epsilon|$, $|V_{cb}|$, $|V_{ub}/V_{cb}|$, ΔM_d, $\tau(B_d)$, $\overline{m_t}$. The fits can be used to exclude extreme values of the pseudoscalar coupling constants, with the range 130 MeV $< f_{B_d}\sqrt{\hat{B}_{B_d}} <$ 250 MeV still allowed for $\hat{B}_K = 0.75$, although the fits at the two boundary values of $f_{B_d}\sqrt{\hat{B}_{B_d}}$ are poor.

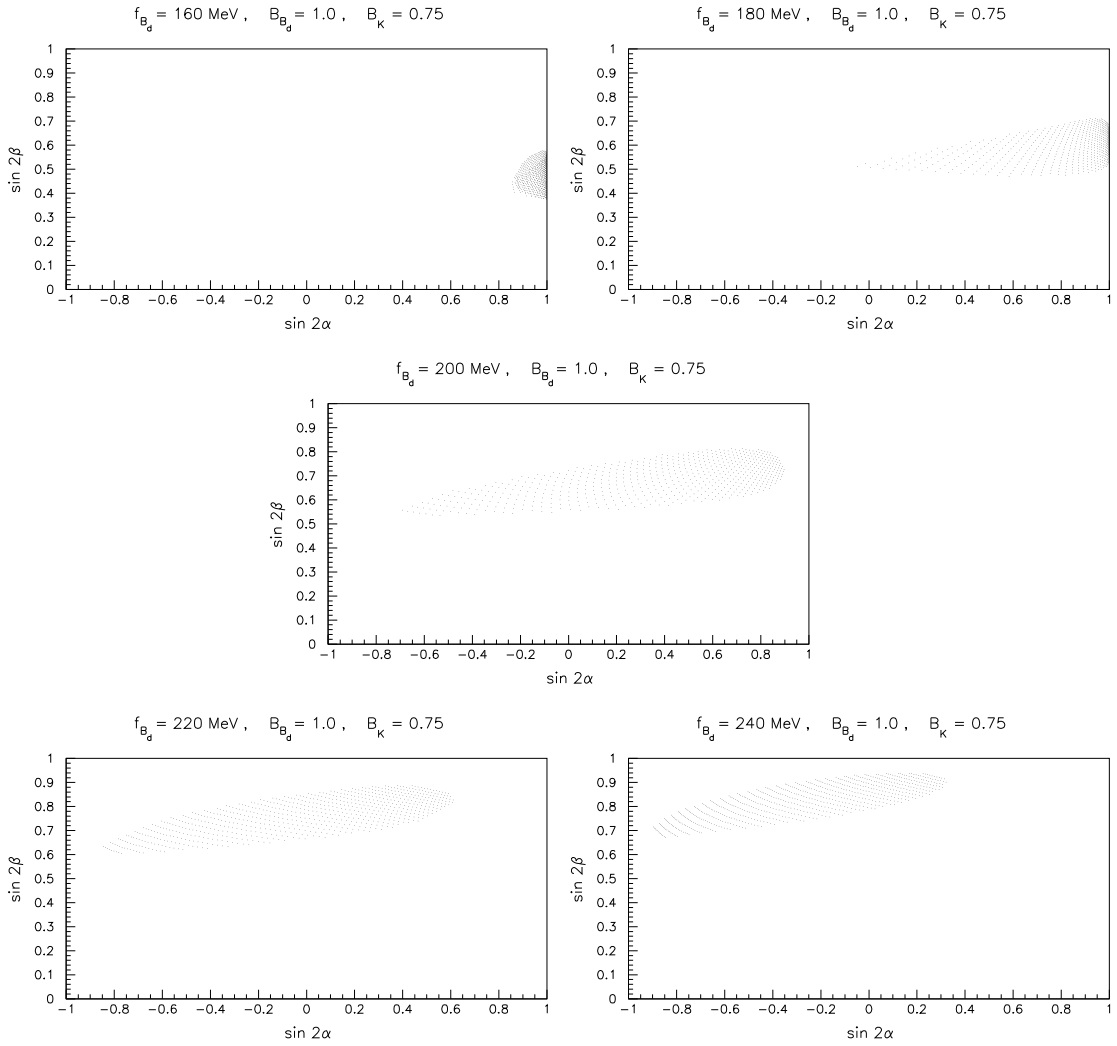

Figure 7: Allowed region of the CP asymmetries $\sin 2\alpha$ and $\sin 2\beta$ resulting from the "experimental fit" of the data for different values of the coupling constant $f_{B_d}\sqrt{\hat{B}_{B_d}}$ indicated on the figures a) – e). We fix $\hat{B}_K = 0.75$.

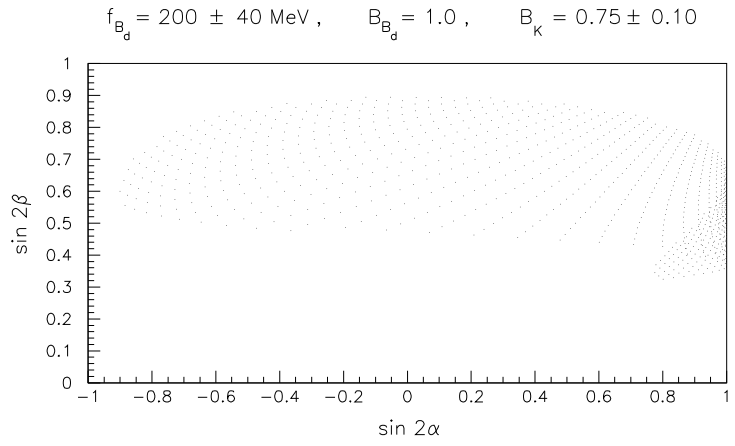

Figure 8: Allowed region of the CP-violating quantities $\sin 2\alpha$ and $\sin 2\beta$ resulting from the "combined fit" of the data for the ranges for $f_{B_d}\sqrt{\hat{B}_{B_d}}$ and $\hat{B}_K$ given in the text.

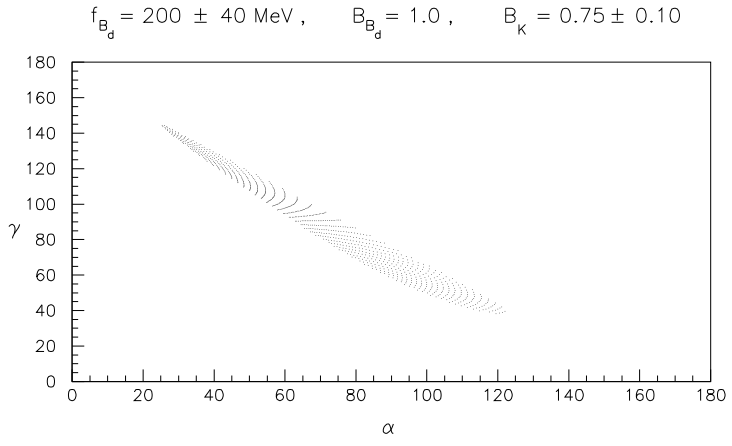

Figure 9: Allowed values (in degrees) of the angles α and γ resulting from the "combined fit" of the data for the ranges for $f_{B_d}\sqrt{\hat{B}_{B_d}}$ and $\hat{B}_K$ given in the text.

(ii) The newest experimental and theoretical numbers restrict the allowed CKM unitarity triangle in the (ρ, η)-space considerably more than before. However, the present uncertainties are still large – despite the new, more accurate experimental data, our knowledge of the unitarity triangle is still deficient. This underscores the importance of measuring CP-violating rate asymmetries in the B system. Such asymmetries are largely independent of theoretical hadronic uncertainties, so that their measurement will allow us to accurately pin down the parameters of the CKM matrix. Furthermore, unless our knowledge of the pseudoscalar coupling constants improves considerably, better measurements of such quantities as x_d will not help much in constraining the unitarity triangle. On this point, help may come from the experimental front. It may be possible to measure the parameter f_{B_d}, using isospin symmetry, via the charged-current decay $B_u^\pm \to \tau^\pm \nu_\tau$. Along the same lines, the prospects for measuring (f_{B_d}, f_{B_s}) in the FCNC leptonic and photonic decays of B_d^0 and B_s^0 hadrons, $(B_d^0, B_s^0) \to \mu^+\mu^-, (B_d^0, B_s^0) \to \gamma\gamma$ in future B physics facilities are not entirely dismal [42].

(iii) We have determined bounds on the ratio $|V_{td}/V_{ts}|$ from our fits. For 130 MeV $\leq f_{B_d}\sqrt{\hat{B}_{B_d}} \leq 250$ MeV, i.e. in the entire allowed domain, at 95 % C.L. we find

$$0.15 \leq \left|\frac{V_{td}}{V_{ts}}\right| \leq 0.34 \ . \tag{31}$$

These bounds are now better than those obtained from unitarity, which gives $0.11 \leq |V_{td}/V_{ts}| \leq 0.33$. Furthermore, the upper bound from our analysis is more restrictive than the current experimental upper limit following from the CKM-suppressed radiative penguin decays $BR(B \to \omega + \gamma)$ and $BR(B \to \rho + \gamma)$, which at present yield at 90% C.L. [43]

$$\left|\frac{V_{td}}{V_{ts}}\right| \leq 0.45 - 0.56 \ , \tag{32}$$

depending on the model used for the SU(3)-breaking in the relevant form factors [44]. Long-distance effects in the decay $B^\pm \to \rho^\pm + \gamma$ may introduce theoretical uncertainties comparable to those in the SU(3)-breaking part but the corresponding effects in the decays $B^0 \to (\rho^0, \omega) + \gamma$ are expected to be very small [45].

(iv) Using the measured value of m_t, we find

$$x_s = (19.5 \pm 3.3)\, \frac{f_{B_s}^2 \hat{B}_{B_s}}{(230 \text{ MeV})^2} \ . \tag{33}$$

Taking $f_{B_s}\sqrt{\hat{B}_{B_s}} = 230$ (the central value of lattice-QCD estimates), and allowing the coefficient to vary by $\pm 2\sigma$, this gives

$$12.9 \leq x_s \leq 26.1 \ . \tag{34}$$

No reliable confidence level can be assigned to this range – all that one can conclude is that the SM predicts large values for x_s, which lie mostly

above the LEP 95% C.L. lower limit of $\Delta M_s > 9.2\ (ps)^{-1}$, which on using $\tau(B_s) = 1.52\ ps$ gives $x_s > 14.0$.

(v) The ranges for the CP-violating rate asymmetries parametrized by $\sin 2\alpha$, $\sin 2\beta$ and and $\sin^2\gamma$ are determined at 95% C.L. to be

$$\begin{aligned} -0.90 \leq \sin 2\alpha \leq 1.0\ , \\ 0.32 \leq \sin 2\beta \leq 0.94\ , \\ 0.34 \leq \sin^2\gamma \leq 1.0\ . \end{aligned} \tag{35}$$

Penguin amplitudes may play a significant role in some methods of extracting the CKM phases. Their magnitude, relative to the tree contribution, is therefore of some importance. One factor in determining this relative size is the ratio of CKM matrix elements $|V_{td}/V_{ub}|$. We find

$$1.4 \leq \left|\frac{V_{td}}{V_{ub}}\right| \leq 4.6\ . \tag{36}$$

Acknowledgements:

We thank Roger Forty, Lawrence Gibbons, Guido Martinelli, Hans-Guenther Moser, Stephan Narison, Sheldon Stone, Ed Thorndike and Christian Zeitnitz for very helpful discussions. Some experimental results used in these CKM fits have been kindly communicated to us by Lawrence Gibbons. A.A. thanks Stephan Narison for the hospitality in Montpellier during the conference QCD '96.

References

[1] N. Cabibbo, Phys. Rev. Lett. **10** (1963) 531; M. Kobayashi and K. Maskawa, Prog. Theor. Phys. **49** (1973) 652.

[2] A. Ali and D. London, preprint DESY 95-148, UdeM-GPP-TH-95-32 [hep-ph/9508272], to appear in the *Proc. of the 6th Int. Symp. on Heavy Flavour Physics*, Pisa, June 6-9, 1995.

[3] L. Wolfenstein, Phys. Rev. Lett. **51** (1983) 1945.

[4] A. Ali and D. London, *Z. Phys.,* C65 (1995) 431.

[5] R.M. Barnett et al. (Particle Data Group), Phys. Rev. **D54** (1996) 1.

[6] Th. Müller, Plenar Votrag auf der Frühjahrstagung 1996 der deutschen Physikalischen Gesellschaft - Sektion Teilchenphysik, Hamburg, FRG, März 18-21, 1996.

[7] N. Gray, D.J. Broadhurst, W. Grafe, and K. Schilcher, Z. Phys. **C48** (1990) 673.

[8] M. Neubert, Preprint CERN-TH/95-107 [hep-ph/9505238].

[9] M. Shifman, Preprint TPI-MINN-95/15-T [hep-ph/9505289].

[10] T. Skwarnicki, preprint [hep-ph/9512395], to appear in the *Proc. of the 17th Int. Symp. on Lepton Photon Interactions*, Beijing, P.R. China, August 1995.

[11] N. Isgur and M.B. Wise, *Phys. Lett.,* B232 (1989) 113; 237 (1990) 527.

[12] L. Gibbons (CLEO Collaboration), Invited talk at the International Conference on High Energy Physics, Warsaw, ICHEP96 (1996).

[13] A. Czarnecki, Phys. Rev. Lett. **76** (1996) 4124.

[14] M.E. Luke, *Phys. Lett.,* B252 (1990) 447.

[15] M. Gremm, A. Kapustin, Z. Ligeti, and M.B. Wise, preprint CALT-68-2043 [hep-ph/9603314].

[16] J. Bartelt et al. (CLEO Collaboration), Phys. Rev. Lett. **64** (1990) 16.

[17] A.J. Buras, W. Slominski, and H. Steger, Nucl. Phys. **B238** (1984) 529; *ibid.* **B245** (1984) 369.

[18] S. Herrlich and U. Nierste, Nucl. Phys. **B419** (1994) 292.

[19] A.J. Buras, M. Jamin and P.H. Weisz, Nucl. Phys. **B347** (1990) 491.

[20] S. Herrlich and U. Nierste, Phys. Rev. **D52** (1995) 6505.

[21] A. Soni, preprint [hep-lat/9510036] (1995).

[22] J. Bijnens and J. Prades, Nucl. Phys. **B444** (1995) 523.

[23] S. Sharpe, Nucl. Phys. B (Proc. Suppl.) **34** (1994) 403.

[24] M. Crisafulli et al. (APE Collaboration), Phys. Lett. **B369** (1996) 325.

[25] S. Aoki et al. (JLQCD Collaboration), preprint UTHEP-322 (1995) [hep-lat/9510012]. The numbers cited for B_K from the JLQCD collaboration as well as from the work of Soni and Bernard are quoted by Soni in his review [21].

[26] C. Zeitnitz, invited talk at the 4th International Workshop on B-Physics at Hadron Machines (BEAUTY 96), Rome, 17-21 June, 1996, and private communication.

[27] H. Wittig, Invited talk presented at the III German-Russian Workshop on Heavy Quark Physics, Dubna, Russia, 20-22 May, 1996, [hep-ph/9606371].

[28] A.K. Ewing et al. (UKQCD Collaboration), preprint, [hep-lat-9508030] (1995).

[29] R. Petronzio (ALPHA Collaboration), private communication.

[30] S. Narison, Phys. Lett. **B351** (1995) 369.

[31] Sau Lan Wu, preprint WISC-EX-96-343 [hep-ex/9602003], to appear in the *Proc. of the 17th Int. Symp. on Lepton and Photon Interactions*, Beijing, P.R. China, August 1995.

[32] "Combined limit on the B_s^0 oscillation frequency", contributed paper by the ALEPH collaboration to the International Conference on High Energy Physics, Warsaw, ICHEP96 PA08-020 (1996).

[33] For reviews, see, for example, Y. Nir and H.R. Quinn, in *B Decays*, edited by S. Stone (World Scientific, Singapore, 1992) 362; I. Dunietz, *ibid* 393.

[34] R. Aleksan, B. Kayser, and D. London, Phys. Rev. Lett. **B73** (1994) 18.

[35] S. Narison, Phys. Lett. **B322** (1994) 247; S. Narison and A. Pivovarov, *ibid* **B327** (1994) 341.

[36] J. Richman, plenary talk at the International Conference on High Energy Physics, Warsaw, ICHEP96 (1996).

[37] D. London and R. Peccei, Phys. Lett. **B223** (1989) 257; B. Grinstein, Phys. Lett. **B229** (1989) 280; M. Gronau, Phys. Rev. Lett. **63** (1989) 1451, Phys. Lett. **B300** (1993) 163.

[38] M. Gronau and D. London, Phys. Rev. Lett. **65** (1990) 3381.

[39] R. Aleksan, I. Dunietz, and B. Kayser, Z. Phys. **C54** (1992) 653.

[40] M. Gronau and D. Wyler, Phys. Lett. **B265** (1991) 172. See also M. Gronau and D. London, Phys. Lett. **B253** (1991) 483; I. Dunietz, Phys. Lett. **B270** (1991) 75.

[41] A.S. Dighe, M. Gronau and J.L. Rosner, CERN-TH/96-68, hep-ph/9604233, to be published in *Phys. Rev.* **D**.

[42] A. Ali, preprint DESY 96-106 [hep-ph/9606324]; to appear in the Proceedings of the XX International Nathiagali Conference on Physics and Contemporary Needs, Bhurban, Pakistan, June 24-July 13, 1995 (Nova Science Publishers, New York, 1996).

[43] R. Ammar et al. (CLEO Collaboration), CLEO CONF 96-05, ICHEP96 PA05-093 (1996).

[44] A. Ali, V.M. Braun and H. Simma, Z. Phys. **C63** (1994) 437; J.M. Soares, Phys. Rev. **D49** (1994) 283; S. Narison, Phys. Lett. **B327** (1994) 354.

[45] A. Ali and V.M. Braun, Phys. Lett. **B359** (1995) 223; A. Khodzhamirian, G. Stoll, and D. Wyler, Phys. Lett. **B358** (1995) 129.